

# Sulfidation of nanoscale zerovalent iron in the presence of two organic macromolecules and its effects on trichloroethene degradation

Sourjya Bhattacharjee, Subhasis Ghoshal\*

Department of Civil Engineering, McGill University, Montreal, QC H3A 0C3, Canada

## SUPPORTING INFORMATION

\*Corresponding author phone: 514-398-6867; fax: 514-398-7361; email: [subhasis.ghoshal@mcgill.ca](mailto:subhasis.ghoshal@mcgill.ca)

### Optimizing sulfide dose:

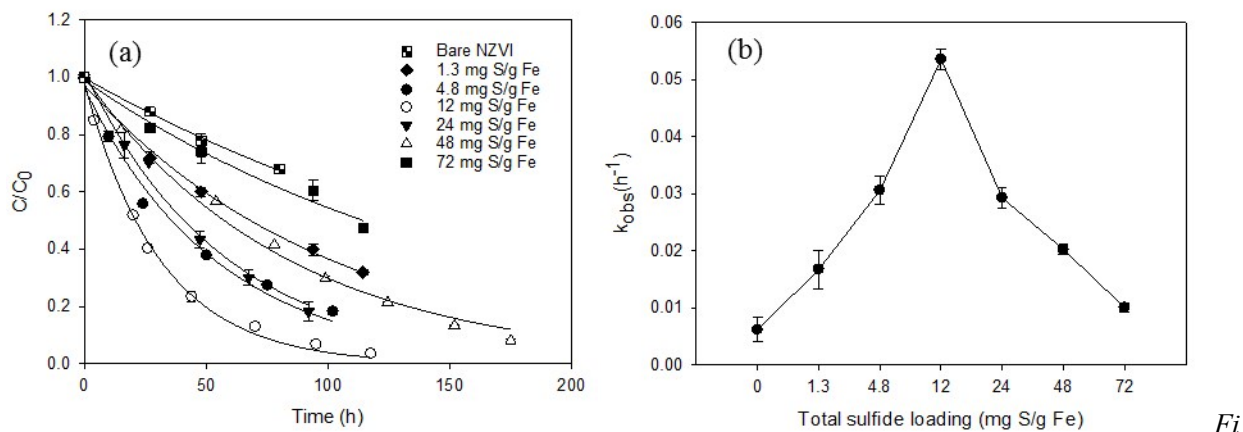


Figure S1: (a) Effect of sulfide loading (mg S/g Fe) on TCE degradation in systems containing NZVI at 0.18 g/L (= 0.153 g/L Fe). Initial TCE concentration was 0.11 mM. (b) Pseudo first order TCE degradation rate constants. Errors bars indicate standard deviations of triplicate measurements.

Varying concentrations of Na<sub>2</sub>S were added to NZVI suspensions and consequently tested for TCE dechlorination to determine the optimum Na<sub>2</sub>S dose (Figure S1). 2.31 mM Na<sub>2</sub>S (10.3 mg S/g NZVI) provided the highest TCE degradation rate with  $k_{obs} = 0.055 \text{ h}^{-1}$  and was thus the optimum Na<sub>2</sub>S dose. Therefore all NZVI particles used in reactivity experiments in the manuscript were sulfidated at the total Na<sub>2</sub>S dose of 2.31 mM. At the optimum dose of Na<sub>2</sub>S added, 54% of total sulfide added was deposited on the particle (= 5.53 mg S/g NZVI).

### XPS:

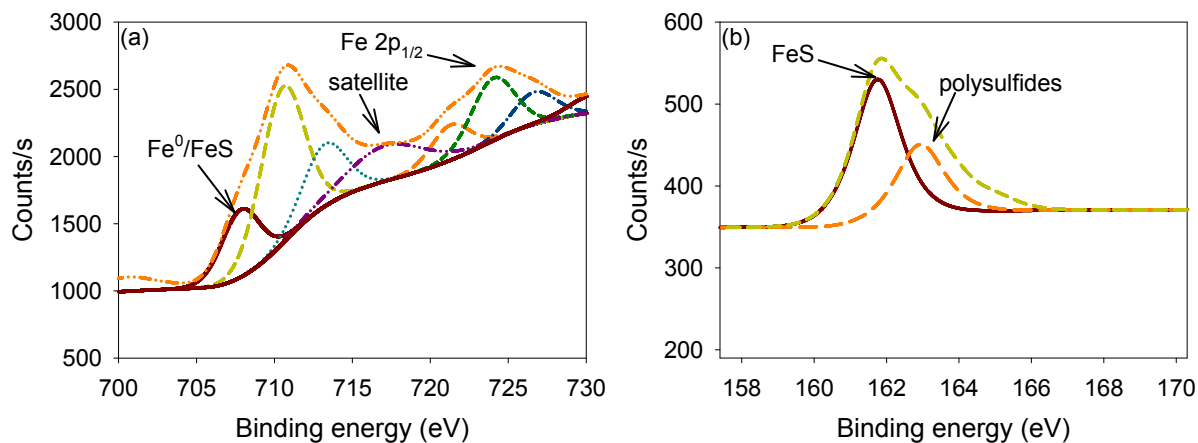
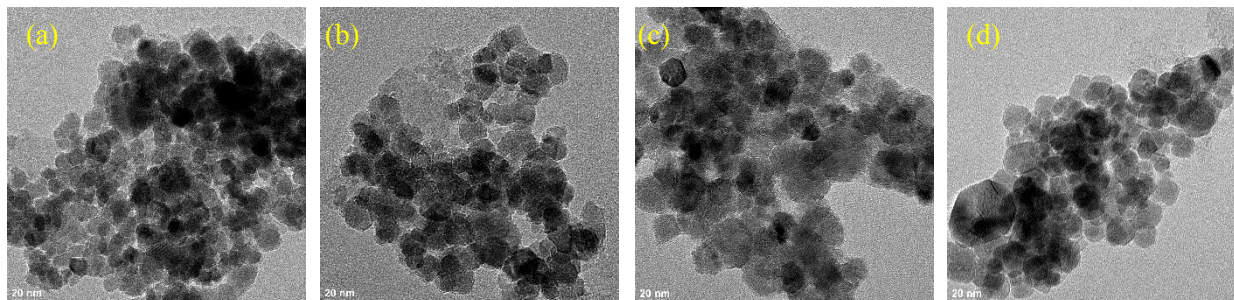
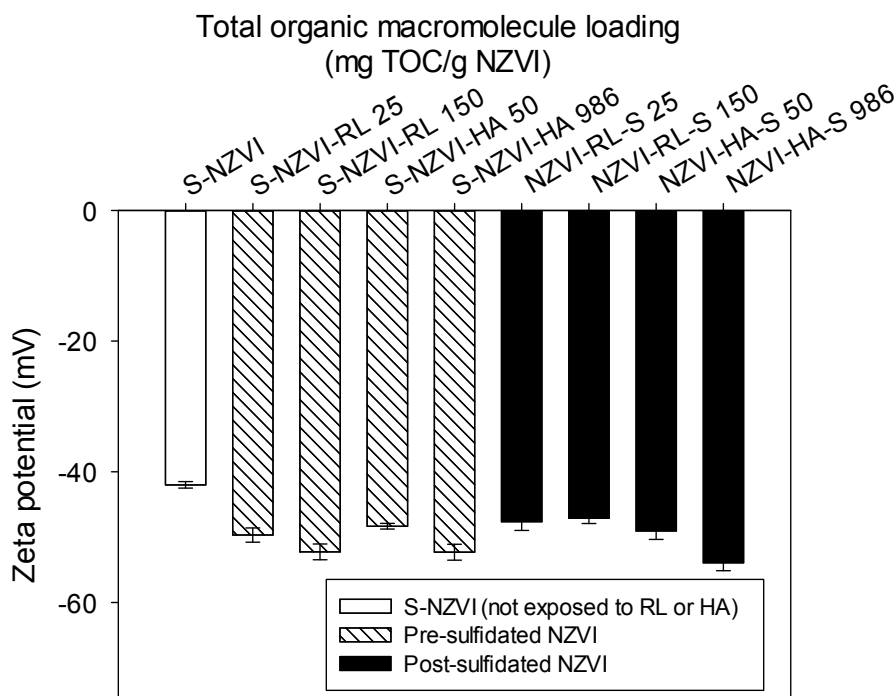


Figure S2: (a) Narrow scans of Fe 2p spectra and various resolved peaks for S-NZVI (b) Narrow scans of S 2p spectra and various resolved peaks for S-NZVI

Low resolution scans for S-NZVI indicated the presence of Fe, O and S on the surface. A high resolution Fe 2p spectra of the sample (Figure S2a) reveals deconvoluted Fe 2p<sub>3/2</sub> spectral peaks at 707.4 which can be attributed to Fe<sup>0</sup>, as well as iron monosulfide (as discussed below)<sup>1</sup>. Peaks at 710.5 eV and 713.3 eV are attributed to Fe<sup>3+</sup> oxidation state (Fe<sub>2</sub>O<sub>3</sub>, FeOOH).<sup>2</sup> Oxygen assignments for the high resolution spectra O1s (data not shown) indicate peaks at 530.2 and 531.7 eV which also confirm the presence of iron oxides and hydroxides. High resolution peaks for S 2p<sub>3/2</sub> spectra for the sample (Figure S2b) shows peaks at 161.5 eV indicating presence of FeS<sup>1</sup> and at 163.0 eV indicating polysulfide (S<sub>n</sub><sup>2-</sup>) and Fe(III) interaction.<sup>3</sup>



**Figure S3:** TEM images of (a) S-NZVI-RL (b) S-NZVI-HA (c) NZVI-RL-S (d) NZVI-HA-S. Concentration of RL was 50 mg TOC/g NZVI and HA was 150 mg TOC/g NZVI.



**Figure S4:** Zeta potential values for pre-sulfidated, post-sulfidated and sulfidated NZVI not exposed to organic molecules, measured in 3mM NaCl ionic strength. Numerical values on X axis represent the the total loading of the organic molecule in mg TOC/g NZVI.

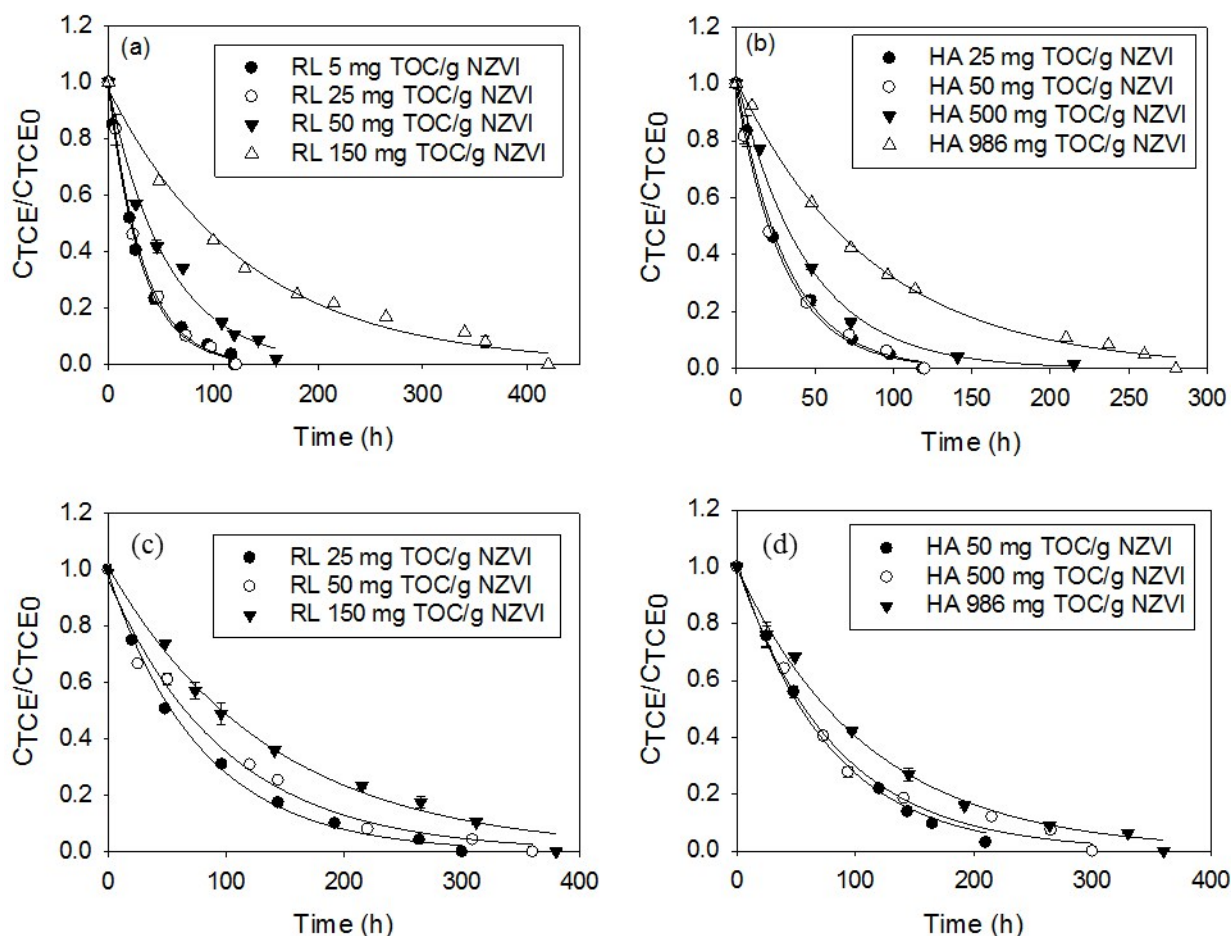


**Figure S5:** TCE degradation profile (a) S-NZVI-RL (b) S-NZVI-HA (c) NZVI-RL-S (d) NZVI-HA-S

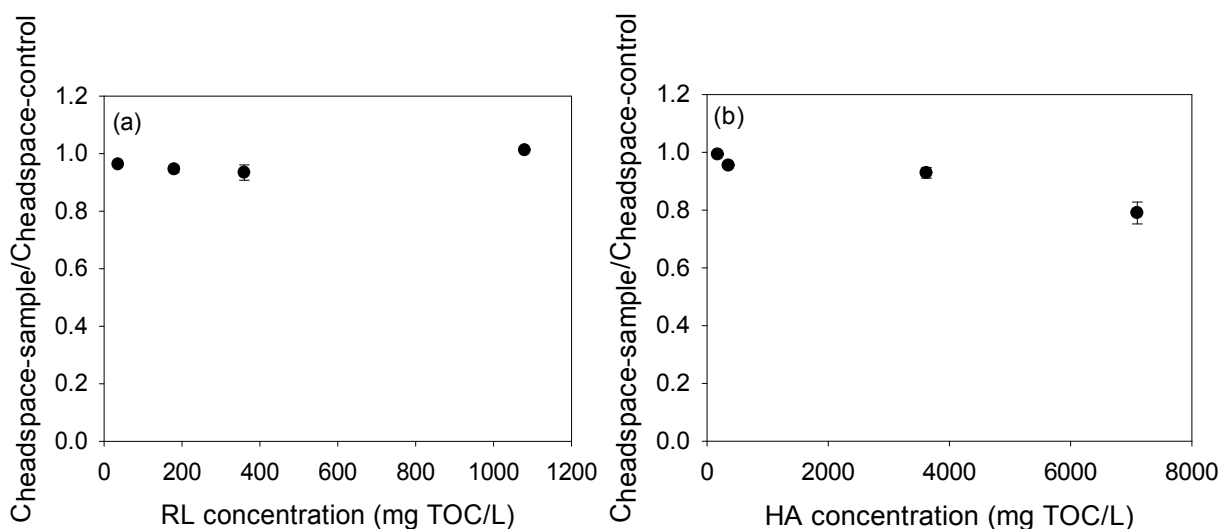
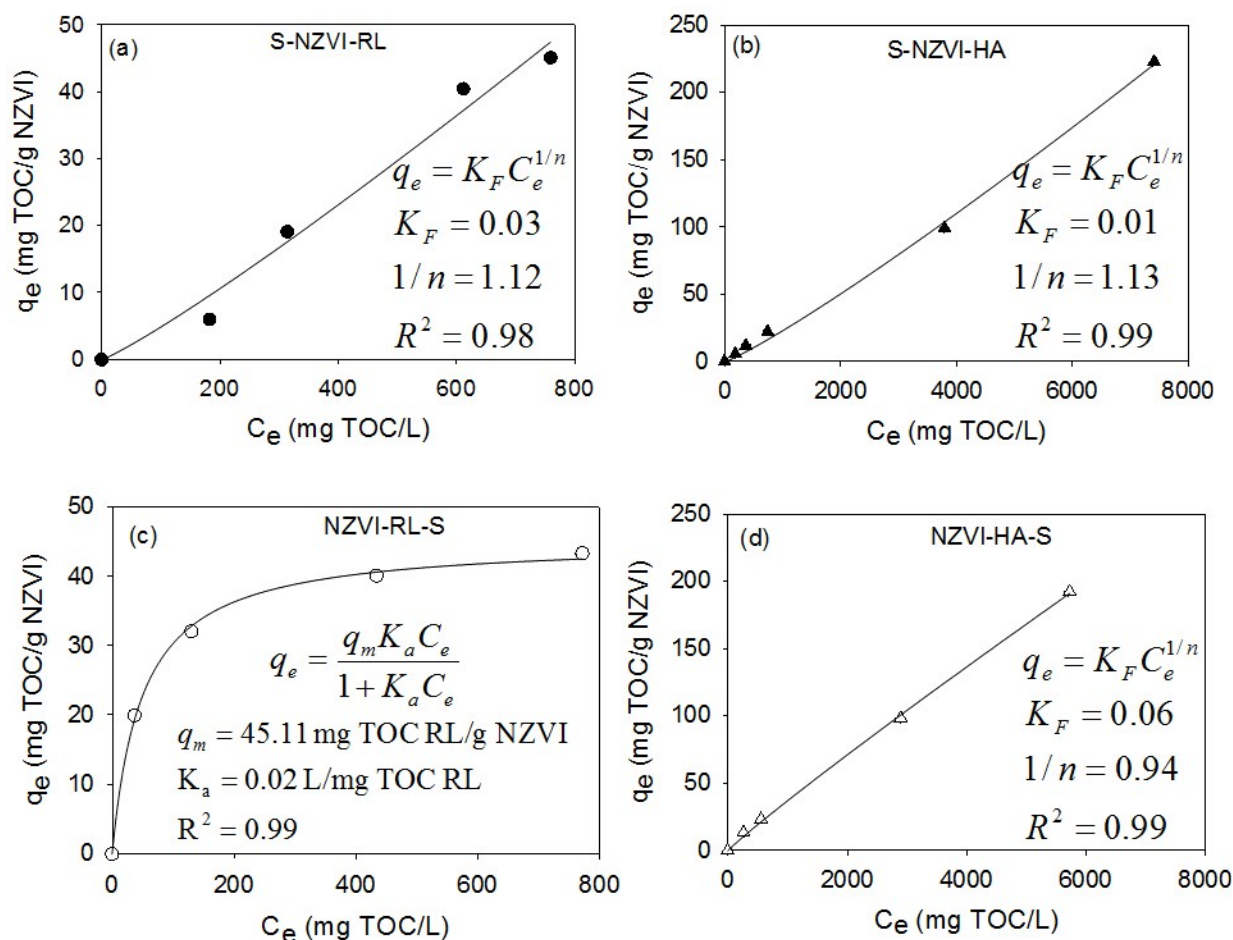


**Figure S6:** Partitioning of TCE in (a) RL only solutions (b) HA only solutions

Figure S6b shows that as the concentration of HA increases in solution, the amount of TCE partitioning into the solution increases, thereby decreasing the headspace TCE concentrations.



F

**figure S7:** (a) RL adsorption in S-NZVI-RL fitted with the Freundlich isotherm, where  $K_F$  and  $n$  are empirical constants. (b) HA adsorption in S-NZVI-HA fitted with the Freundlich isotherm (c) RL adsorption in NZVI-RL-S fitted with Langmuir isotherm, where  $q_e$  is the equilibrium adsorption capacity of NZVI,  $C_e$  is the equilibrium aqueous phase concentration of RL,  $q_m$  is the maximum adsorption capacity of NZVI and  $K_a$  is the adsorption equilibrium constant (d) HA adsorption in NZVI-HA-S fitted with Freundlich isotherm

**Differences in sorption isotherms.** It is evident that the adsorption profile of RL in S-NZVI-RL (Figure S7a) was significantly different from NZVI-RL-S (Figure S7c). For instance, at a total RL loading of 50 mg TOC/g NZVI, 15 mg TOC/g NZVI of RL was adsorbed in S-NZVI-RL, whereas almost twice as much RL was adsorbed to NZVI (32 mg TOC/g NZVI) in NZVI-RL-S. Because the solution pH was the same under both scenarios, the difference in sorption behavior is attributed to the surface chemistry of the nanoparticles. The presence of sulfide surface sites on S-NZVI may have resulted in lower affinity of RL compared to the iron oxides/hydroxides on NZVI. The sorption isotherms could be qualitatively described using Langmuirian and Freundlich isotherms as shown in figure S7a & S7c. The adsorption of HA under S-NZVI-HA (Figure S7b) and NZVI-HA-S (Figure S7d) scenarios did not display distinctively different sorption behaviors. Both qualitatively displayed Freundlich isotherms. It is likely that the sorption behavior of HA is primarily driven by its molecular configuration (which is dependent on its macromolecular structure).

## FTIR analysis:

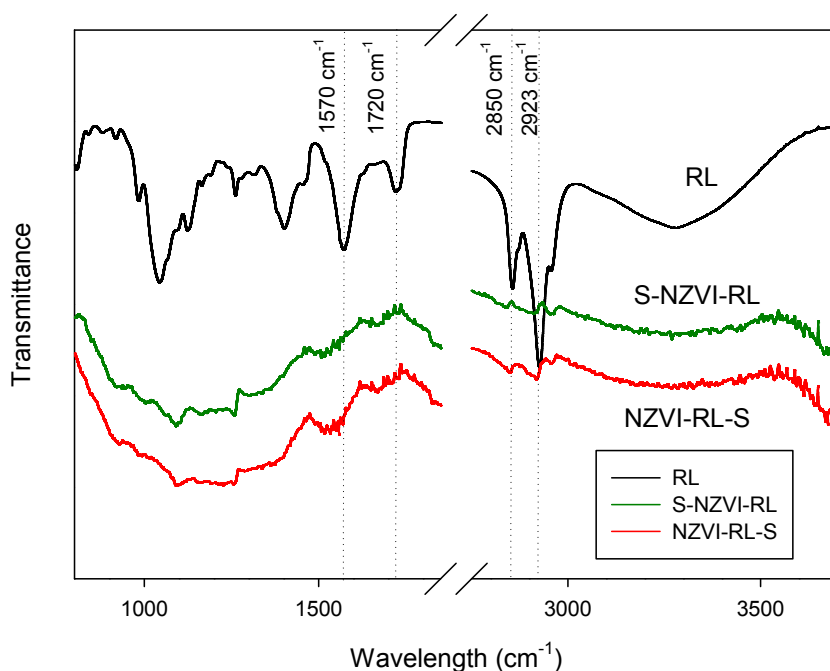


**Figure S8:** FTIR spectra of RL, S-NZVI-RL and NZVI-RL-S

**RL spectra:** The major peaks at 2920 and 2850  $\text{cm}^{-1}$  are the  $\nu_{\text{asym}}(\text{CH}_2)$  and  $\nu_{\text{sym}}(\text{CH}_2)$  modes respectively. The low frequency region is dominated by the carboxylic acid  $\nu_{\text{sym}}(\text{C}=\text{O})$  stretch at 1720  $\text{cm}^{-1}$  and the  $\nu_{\text{asym}}(\text{COO}^-)$  carboxylate mode at 1570  $\text{cm}^{-1}$ . The region below 1500  $\text{cm}^{-1}$  corresponds to the fingerprint region for rhamnolipid which includes vibrational modes of the rhamnose head group.<sup>4, 5</sup>

**S-NZVI-RL and NZVI-RL-S:** The spectra for RL sorbed in S-NZVI-RL and NZVI-RL-S were nearly identical. The peak positions of asymmetric and symmetric  $\text{CH}_2$  did not change significantly. However the  $\nu_{\text{asym}}(\text{COO}^-)$  carboxylate mode shifted to 1520  $\text{cm}^{-1}$  while the peak at  $\nu_{\text{sym}}(\text{C}=\text{O})$  shifted to 1670  $\text{cm}^{-1}$ . Overall it appears, that the interaction of rhamnolipid at the NZVI surface and S-NZVI surface is through the carboxyl group.

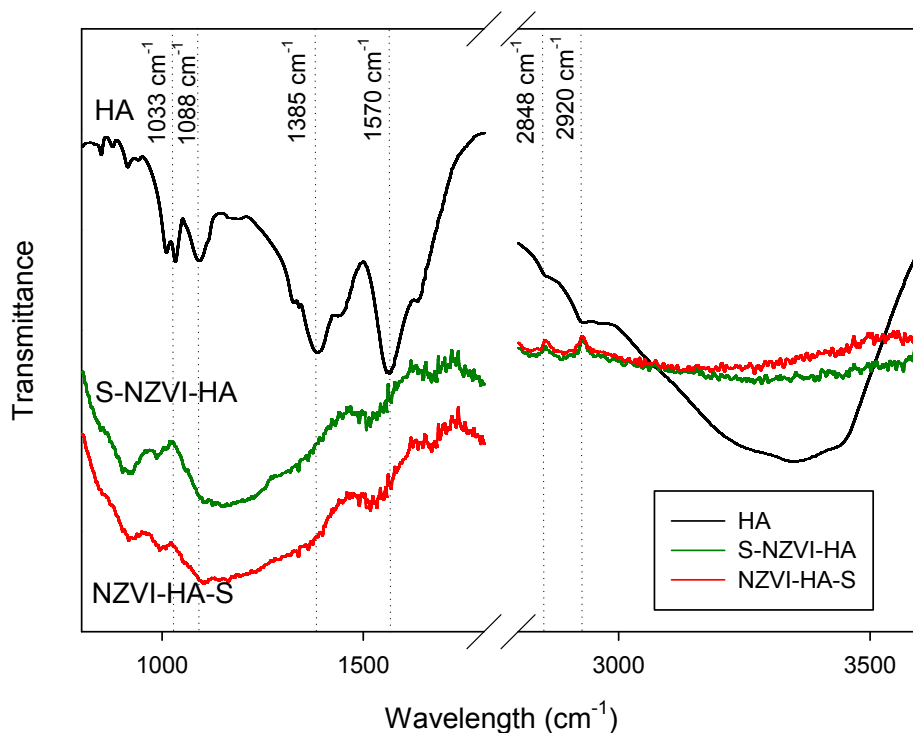


**Figure S9:** FTIR spectra of HA, S-NZVI-HA and NZVI-HA-S

**HA spectra:** The wide peak at 3354 cm<sup>-1</sup> is attributed to hydrogen bonding and O-H stretching while peaks at 2920 and 2848 cm<sup>-1</sup> are due to C-H stretch of aliphatic groups. Peaks at 1570 cm<sup>-1</sup> can be attributed to aromatic C=C, at 1385 cm<sup>-1</sup> to symmetric stretching of COO<sup>-</sup> and C-OH stretching of phenolic OH. Peaks for C-O stretching of carbohydrate or alcohol are observed at 1088 & 1033 cm<sup>-1</sup>.<sup>16, 7</sup>

**S-NZVI-HA and NZVI-HA-S:** After sorption, significant peak shifts were observed at stretching modes of C=C (1670 cm<sup>-1</sup>) and COO<sup>-</sup> or phenolic OH (1510 cm<sup>-1</sup>). This suggests that the aromatic COOH and hydroxyl or phenolic OH are the main functional groups that interact with the NZVI and S-NZVI surfaces.

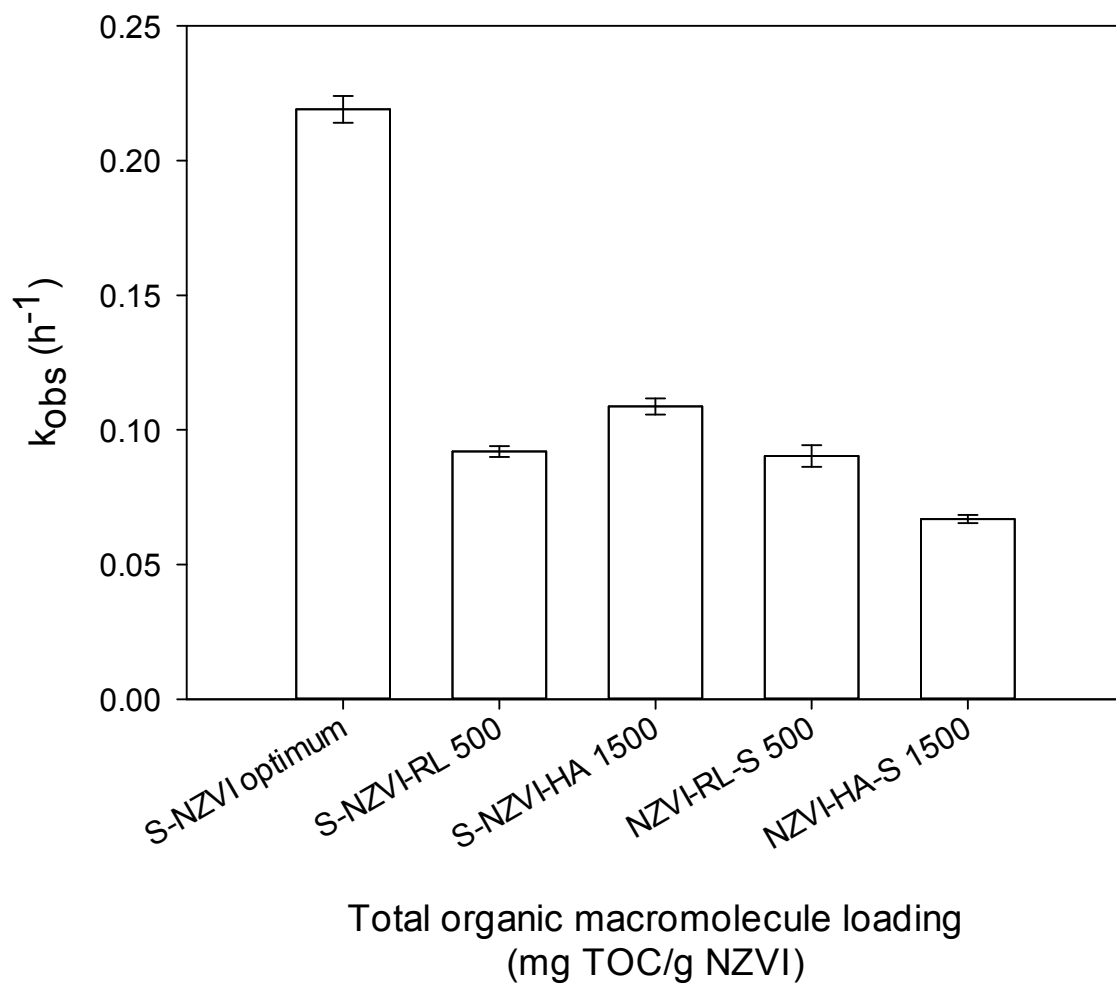


**Figure S10:** TCE degradation rate constants for NZVI synthesised through borohydride reduction of iron sulfate salt and then sulfidated using  $Na_2S$ . Numerical values on X axis represent the total loading of the organic molecule in mg TOC/g NZVI. 'S-NZVI optimum' is the NZVI (not exposed to HA/RL) dosed with sulfide for optimum reactivity to TCE. This was obtained from values reported by Rajajayavel et al.<sup>1</sup> for 1.5 g/L of NZVI BET surface area of 25 m<sup>2</sup>/g.

## References

1. S. R. C. Rajajayavel and S. Ghoshal, *Water research*, 2015, **78**, 144-153.
2. M. Descostes, F. Mercier, N. Thromat, C. Beaucaire and M. Gautier-Soyer, *Applied Surface Science*, 2000, **165**, 288-302.
3. R. B. Herbert, S. G. Benner, A. R. Pratt and D. W. Blowes, *Chemical Geology*, 1998, **144**, 87-97.
4. A. Lebron-Paler, *Solution and Interfacial Characterization of Rhamnolipid Biosurfactant from Pseudomonas aeruginosa ATCC 9027*, ProQuest, 2008.
5. F. Leitermann, C. Syldatk and R. Hausmann, *Journal of biological engineering*, 2008, **2**, 1-8.
6. L. Xie and C. Shang, *Environmental science & technology*, 2005, **39**, 1092-1100.
7. A. B. Giasuddin, S. R. Kanel and H. Choi, *Environmental Science & Technology*, 2007, **41**, 2022-2027.